

Charge-Based Isolation of Extracellular Vesicles from Human Plasma

Woojin Back, Minseo Bang, Jik-Han Jung, Ka-Won Kang, Byeong Hyeon Choi, Yeonho Choi, Sunghoi Hong, Hyun Koo Kim, Yong Park, and Ji-Ho Park*

Cite This: *ACS Omega* 2024, 9, 17832–17838

Read Online

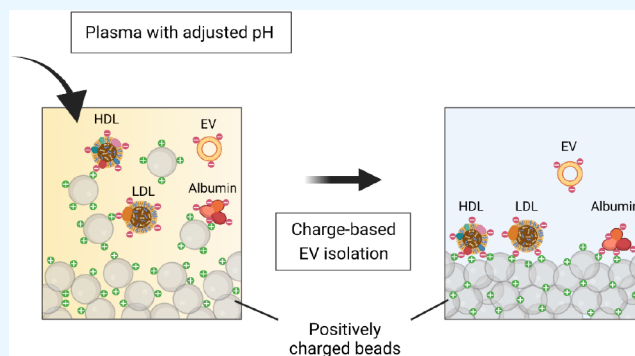
ACCESS |

Metrics & More

Article Recommendations

Supporting Information

ABSTRACT: Extracellular vesicles (EVs) have garnered significant attention due to their potential applications in disease diagnostics and management. However, the process of isolating EVs, primarily from blood samples, is still suboptimal. This is mainly attributed to the abundant nature of soluble proteins and lipoproteins, which are often separated together with EVs in the end products of conventional isolation methods. As such, we devise a single-step charge-based EV isolation method by utilizing positively charged beads to selectively remove negatively charged major impurities from human plasma via electrostatic interaction. By carefully controlling the buffer pH, we successfully collected EVs from undesired plasma components with superior purity and yield compared to conventional EV collection methods. Moreover, the developed process is rapid, taking only about 20 min for overall EV isolation. The charge-based isolation can ultimately benefit the EV-based liquid biopsy field for the early diagnosis of various diseases.



1. INTRODUCTION

Extracellular vesicles (EVs) are membranous vesicles released by all cell types.¹ EVs can be subcategorized into exosomes, which originate from multivesicular bodies (MVBs) and microvesicles (MVs) that are formed by plasma membrane shedding. The diameter of exosomes falls in the range between 30 and 150 nm while MVs range from 40 nm to 1 μm .^{2,3} EVs are found in bodily fluids, including blood, lymph, ascites, cerebrospinal fluid, semen, and breast milk.^{4–9} As EVs carry the information on their parental cell in the form of proteins, lipids, and RNA molecules, they are popularly utilized in liquid biopsies for disease diagnosis and monitoring.¹⁰

However, the field of EV research and clinical translation efforts has been obstructed by the absence of effective standardized EV isolation methods. The International Society for Extracellular Vesicles (ISEV) has therefore highlighted the urgent requirement for establishing more efficient and standardized EV isolation protocols.^{11–14} Although several isolation techniques such as size exclusion chromatography (SEC), polymer precipitation (PP), ultracentrifugation (UC), and density gradient centrifugation methods have been developed for isolating EVs from blood, their wide applications have been hampered by low EV purity mainly due to the presence of soluble proteins and lipoproteins.^{15–21} To be more specific, EV isolation by UC is time-consuming and requires a costly and voluminous device. Moreover, the high g-force associated with UC often leads to the aggregation and disruption of EVs.²² On the other hand, a PP method, which frequently involves polyethylene glycol (PEG), is inexpensive

and allows the rapid isolation of EVs.¹⁴ However, it suffers from drawbacks associated with EV contamination by other plasma constituents and the coisolation of polymers.¹⁴ The same problem also applies to SEC where contamination by similarly sized lipoproteins, which outnumbers EVs by 5- to 6-fold in plasma, is unavoidable.^{14,23} Overall, a low EV yield and the requirement for time-consuming multiple steps associated with current isolation methods augment the need for a new isolation method.

We have designed a charge-based EV isolation method to circumvent the shortfalls associated with currently established EV isolation methods by considering the charge difference between EVs and major impurities present in plasma, such as lipoproteins and albumin (Figure 1a). Recent reports revealed that EVs have heterogeneous charge distributions (from highly negative to less negative), and there exists a proportion of EVs with a generally less negative zeta potential, for example, -10 mV, when compared to lipoproteins which have lower average zeta potentials of around -20 mV at pH 7.4.^{21,24,25} In addition, albumin, one of the most abundant protein contaminants in plasma, possesses similar zeta potential to lipoproteins with an isoelectric point (pI) of 4.7.²⁶ Considering such findings, we

Received: September 26, 2023

Revised: March 8, 2024

Accepted: March 27, 2024

Published: April 11, 2024



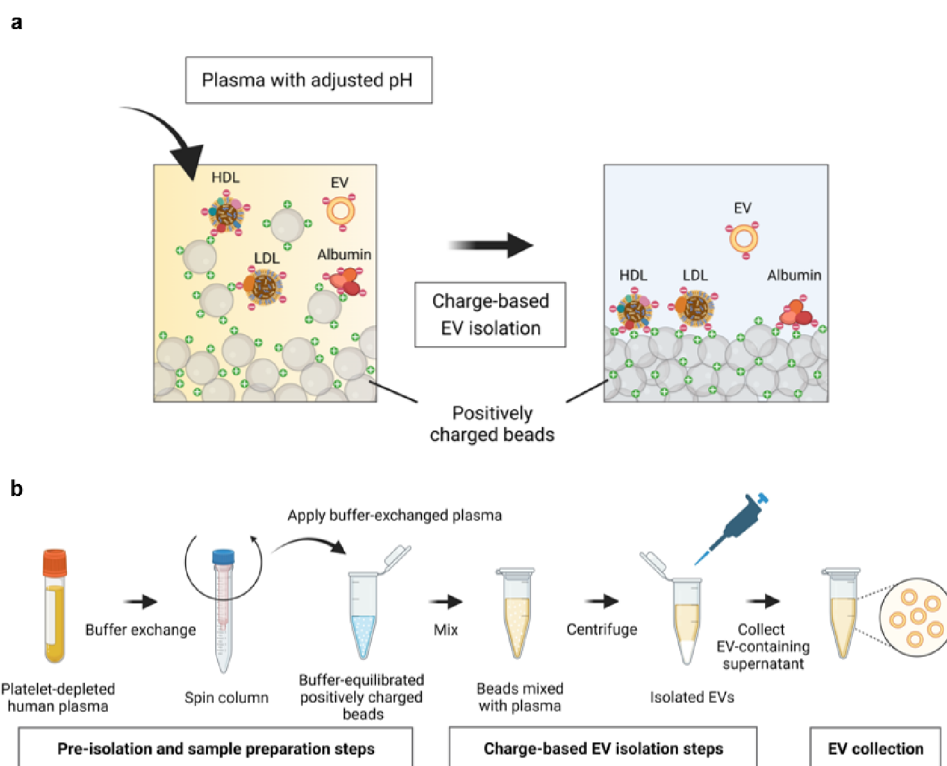


Figure 1. Principle of the charge-based EV isolation process. (a) Charge differences between EVs and major contaminants such as high-density lipoproteins (HDLs), low-density lipoproteins (LDLs), and albumin have been exploited for the isolation process. Buffer pH was carefully optimized to ensure that negatively charged contaminants are selectively bound to positively charged beads while retaining a less negative EV subpopulation in the solution. (b) EV isolation steps involved in the developed charge-based EV isolation process.

utilize a positively charged anion exchange resin to remove highly negative soluble proteins and lipoproteins from a less negatively charged EV subpopulation via electrostatic interaction (Figure 1a). The buffer pH was carefully controlled to attain the maximal purity and yield of isolated EVs (Figure 1b).

2. MATERIALS AND METHODS

2.1. Preparation of Human Plasma. All human blood samples were provided by the Division of Hematology-Oncology and the Department of Internal Medicine, Korea University College of Medicine. Sample preparations were performed as per the guidelines of the Institutional Review Board of Korea University (Anam Hospital) (2020AN0558) and Korea Advanced Institute of Science and Technology (review exempted). All studies were performed in accordance with the Declaration of Helsinki. Blood was collected in trisodium-citrate-containing tubes (BD). Cells and platelets were removed by centrifugation at 10,000g for 30 min at 4 °C.

2.2. Cell Culture. PC-9 and THP-1 cells were respectively cultured in an RPMI 1640 medium supplemented with 10% exosome-depleted fetal bovine serum (dFBS), and 1% (v/v) penicillin and streptomycin. Note that dFBS was prepared by centrifuging FBS for 18 h at 100,000g.¹⁴ EVs were isolated when approximately 80% of cell confluency was reached.

2.3. EV Isolation from Cell Culture Media. Cell culture media were differentially centrifuged at 500g for 10 min, and at 5000g for 30 min, and at 10,000g for 30 min at 4 °C to remove cells, cell debris, apoptotic bodies, and microvesicles. The supernatant was then concentrated 100 times by using an Amicon ultra 100 kDa centrifugal filter (Merck Millipore) and stored at −20 °C.

2.4. EV Collection by Ultracentrifugation. 0.5 mL of platelet-free plasma was diluted with 4 mL of sterile phosphate-buffered saline (PBS) and centrifuged at 100,000g for 1 h at 4 °C by using a Beckman SW60 rotor (Beckman Coulter).¹⁴ Afterward, the supernatant was carefully discarded, and the EV-containing pellet was resuspended in PBS.

2.5. EV Collection by PEG Precipitation. EV was collected by a total exosome isolation (from plasma) kit (Invitrogen). In brief, 0.5 mL of platelet-free plasma was mixed with 0.25 mL of PBS. Afterward, 0.15 mL of exosome precipitation reagent was mixed with the sample and incubated at room temperature for 10 min. After incubation, the mixture was centrifuged at 10,000g for 5 min at room temperature, and the supernatant was carefully discarded. The pellet containing the EVs was then resuspended in PBS.

2.6. EV Collection by Size Exclusion Chromatography (SEC). SEC was performed by using an SEC column filled with 10 mL of Sepharose CL-2B resin (GE Healthcare Life Sciences), according to the previously described protocol.²¹ In brief, 0.5 mL of cell culture medium was loaded onto the SEC column, and 0.5 mL of individual eluate fraction was collected and stored for further downstream analysis.

2.7. Charge-Based EV Isolation. 0.5 mL of platelet-deprived plasma was first buffer exchanged with 10 mM buffers of respective pHs by using a 7 kDa molecular weight cutoff (MWCO) Zeba Spin Desalting Column (Thermo Scientific). A buffer pH of 5.4 was constituted by an acetate buffer, while phosphate buffers were used to prepare the buffers of pH 6.4 and pH 7.4. Buffers of pH 8.4 and 9.4 were formulated with tris and carbonate/bicarbonate buffers, respectively. All buffer concentrations were adjusted to 10 mM in this study.

Simultaneously, 0.5 mL of positively charged anion exchanger, Q Sepharose Fast Flow (Cytiva) was equilibrated with buffers of various pHs. Afterward, 0.5 mL of buffer exchanged plasma was thoroughly mixed with 0.5 mL of buffer-equilibrated positively charged beads left at room temperature for 10 min. The supernatant, which contains unbound plasma components, was then collected, and its osmolarity was made equivalent to 1× PBS by using 10× PBS.

For analysis of plasma constituents that have been bound to positively charged beads, the supernatant which contains the unbound plasma constituents was first removed, and the positively charged beads were washed with DI water 3 times. Afterward, a 1 M NaCl solution was added to the washed beads to detach the entire bound plasma constituents from the positively charged beads.

2.8. SDS-PAGE, Western Blotting, and Protein Concentration Measurement. The amount of proteins present in the isolated samples was determined by bicinchoninic acid (BCA) assay (Thermo Fischer) according to the manufacturer's protocol. For analysis of tetraspanins, such as CD63 and CD9, the samples were mixed with 4× nonreducing LDS sample buffer (Thermo Scientific) while 5× reducing protein sample buffer (Elpis-Biotech) was used for the analysis of non-EV proteins. The samples were then heated for 3 min at 95 °C. Afterward, sodium dodecyl sulfate-polyacrylamide gel electrophoresis (SDS-PAGE) was performed by using a 4–20% gradient polyacrylamide gel (Biorad). Membranes were then transferred to a nitrocellulose membrane by using a Trans-Blot Turbo system (Bio-Rad) and stained with Ponceau S solution (Sigma-Aldrich) for visualization and normalization of protein bands by using a Bio-Rad ChemiDoc imager.

For Western blotting, membranes were blocked with 5 w/v % skim milk in tris-buffered saline supplemented with 0.1 v/v % Tween-20 (TBST) for an hour and incubated with the following primary antibodies overnight at 4 °C: anti-ApoB-100 (1:1000, Santa Cruz Biotechnology, sc-25542), anti-ApoA-1 (1:1000, Abcam, ab33470), anti-CD9 (1:1000, Invitrogen, PA5-85955), anti-CD63 (1:1000, Bioss, bs-1523R), anti-TSG101(1:1000, Bioss, bs-1365R), anti-calnexin (1:1000, Bioss, bs-1693R), and anti-albumin (1:3000, Bioss, bs-0945R). After overnight incubation, the blots were washed at least 5 times by TBST. Primary antibodies were then labeled with horseradish peroxidase (HRP) conjugated anti-rabbit (1:3000, Cell Signaling Technology, 7074S) or anti-mouse (1:3000, Cell Signaling Technology, 7076S) secondary antibodies for 2 h at room temperature with gentle shaking. Afterward, the membranes were washed at least 5 times by TBST and incubated with clarity western ECL buffer (Bio-Rad) for 15 min for HRP detection. Finally, the protein bands were visualized by a Bio-Rad ChemiDoc imager (Bio-Rad), and their intensities were analyzed by using Image Lab Software 5.2 (Bio-Rad). Note that since different proteins have different affinities toward the respective primary antibodies during Western blotting, all analyses and comparisons for the band intensities were made only for the same protein bands.

2.9. Nanoparticle Tracking Analysis (NTA). The size distribution and the number of particles present in the isolated samples were determined by nanoparticle tracking analysis (NTA). In brief, the samples were diluted 10 to 100 times in PBS for subsequent NTA measurements by using a Nanosight instrument (Malvern Instruments) at 25 °C.

2.10. Transmission Electron Microscopy (TEM). Isolated EVs were visualized under TEM according to the previously described method.²¹ In brief, 10 μL of EV sample was mixed with an equal volume of 4% paraformaldehyde (PFA) and incubated on Formvar-carbon-coated electron-microscope grids for 15 min. Next, the grids were washed with PBS and fixed with 2.5% glutaraldehyde for 5 min. The grids were then washed with DI water five times and incubated in phosphotungstic acid (pH 7) for 3 min. Excess stain was removed by blotting with filter paper. The dried grids were then imaged under a field emission transmission electron microscope (FE-TEM, JEM-2100F HR) operating at 200 kV.

2.11. Dynamic Light Scattering (DLS). Dynamic light scattering (DLS) and Zetasizer Nano ZS90 (Malvern Instrument), equipped with a 630 nm solid-state laser, were used to measure the size distributions and zeta potentials of purified EV samples. EV-containing samples were measured without dilution while commercial LDLs (Fitzgerald) and HDLs (Fitzgerald) were measured after a 10-fold dilution in DI water.

3. RESULTS AND DISCUSSION

With the aim of utilizing the electrostatic force of attraction between positively charged resin and non-EV components in the plasma, we first measured the surface charges of EVs and major components in human plasma, including HDLs, LDLs, and albumin, at pH 7.4. We discovered that, in line with previous literature, LDLs exhibited a similar average zeta potential of −23 mV, while HDLs were slightly less negative, with a zeta potential value of approximately −18 mV (Figure S1).^{21,24,25} In addition, albumin, which is the most abundant soluble protein in blood, had a zeta potential of −22 mV, similar to LDLs. The isolated EVs from PC9 and THP-1 cell culture media had zeta potentials of approximately −12.7 and −11.5 mV, respectively. This thus supports the previous literature that the surface charge of EVs is being heterogeneous in nature and there exists a subpopulation of EVs with less negative average zeta potentials in comparison to other highly negative EV subpopulations or non-EV plasma constituents.^{21,24,25}

Based on this finding, we hypothesized that positively charged beads could be utilized to separate a generally less negatively charged EV subpopulation from more negatively charged non-EV components. Note that a “strong” anionic exchanger (Q Sepharose Fast Flow, positive beads) was used for the method development with an aim to keep the number of charges constant regardless of the buffer pH during optimization.²⁷ We varied the buffer pH as this is one of the most critical parameters that influences the electrostatic force of attraction during ion exchange chromatography. To verify whether pH affects protein binding to positively charged beads, we first exchanged and equilibrated 0.5 mL of human plasma and the positively charged beads with 10 mM buffers of various pHs, ranging from 5.4 to 9.4, respectively. A buffer concentration of 10 mM was selected to minimize the effect of ionic strength, which is another parameter that affects ionic interactions during charge-based protein isolation. Afterward, the buffer-exchanged plasma was mixed and vortexed with the positively charged beads and left at room temperature for 10 min. The supernatant, which contains unbound plasma components, was collected, and its ionic strength was immediately made equal to 1× PBS by using 10× PBS. Afterward, the reclaimed supernatant was subjected to a bicinchoninic acid (BCA) assay to quantify the total mass of

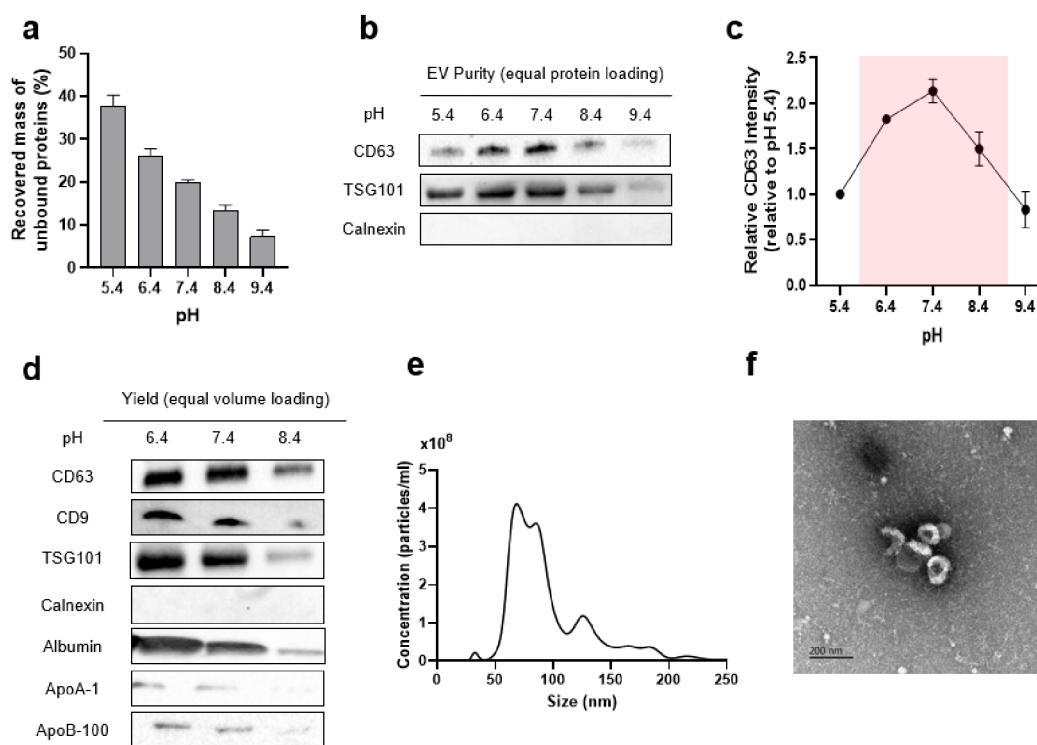


Figure 2. Analyzing the performance of the charge-based EV isolation method. (a) Recovered mass of total unbound protein with respect to pH change (%). (b) EV purity analysis by Western blotting of supernatants collected in (a), which contains unbound plasma constituents (CD63, TSG101, and calnexin (a negative EV marker)). (c) Relative CD63 band intensities obtained in (b), which indicate EV purity. A red box indicates the pH ranges which allow the collection of relatively purer EVs. (d) Yield analysis of EVs (CD63, CD9, TSG101, and calnexin (a negative EV marker)) and plasma impurities (albumin, HDLs (ApoA-1), and LDLs (ApoB-100)) found in the supernatants containing relatively purer EVs as determined in (c). (e) Determination of the size distribution and morphology of EVs collected at pH 7.4 by NTA and (f) TEM, respectively. Data are means \pm s.e.m. [$n = 5$ for (a); $n = 3$ for (b) and (c); $n = 3$ for (d)].

unbound proteins. As expected, an increase in buffer pH resulted in more plasma protein binding to positively charged beads as reflected by the reduction in total protein concentration of the isolated supernatant (Figure 2a).

To precisely monitor the type of proteins removed and observe the possible collection of EVs, the supernatants subjected to charge-based EV isolation methods at different pHs ranging from pH 5.4 to 9.4 were analyzed by Western blotting. Although various EV markers can be utilized for analyzing the purity of EVs isolated, CD63, a tetraspanin protein, was selected as the primary marker for analysis because previous reports revealed that it could be found both on ectosomes and endosome-derived EVs.^{28,29} Equal protein amount from each sample was loaded for Western blotting for the analysis of EV purity.^{15,30} Relatively higher CD63 intensities were observed for EV-containing supernatants isolated at pH ranges 6.4 to 8.4 (Figure 2b,c). On the other hand, weaker CD63 signals were exhibited for pH 5.4 and pH 9.4, respectively. This trend was similar for another EV-associated protein, TSG101. Notably, the highest CD63 band signal was detected at pH 7.4, indicating the isolation of the purest EVs at this pH in comparison to other pHs (Figure 2c). To be more specific, the supernatant subjected to the charge-based EV isolation at pH 7.4 contained at least 2-fold purer EVs when compared to the supernatants collected at pH 5.4 and 9.4 (Figure 2c). Afterward, the same supernatants obtained from pH 6.4 to pH 8.4, each containing relatively purer EV populations, were subjected to Western blotting by equalized volume loading to compare the relative amounts of

contaminants and EVs present in the sample.^{15,30} This analytical method would eventually reveal the information pertinent to protein yield as the amount of protein is equalized when performing the Western blot analysis, as in the case of purity analysis. Similar band intensities were observed for EV-associated markers, specifically CD9 and CD63, demonstrating the presence of similar amounts of EVs (Figure 2d). However, there was a decrease in albumin bands with respect to the pH increase, implying more albumin binding and, thus, its removal at higher pHs. In fact, similar trends were observed for ApoA-1 and ApoB-100 bands which reflect HDLs and LDLs, respectively, even though the decrease in the band intensity with respect to a pH increase was nonlinear (Figure 2d). Overall these results may explain the reason that the plasma sample isolated at pH 7.4 exhibited the highest CD63 purity (Figure 2b,c). In addition, an intensified albumin band was observed by Western blotting with equalized volume loading upon analyzing the bead-bound components of plasma that had undergone charge-based EV isolation at pH 7.4 (Figure S2). On the other hand, a more intensified CD63 band was observed for the supernatant (unbound) sample in comparison to the bead-bound fraction. These results indicate the binding of highly negative EV subpopulations and albumin to positive beads while retaining a less negatively charged EV proportion in solution at a greater amount (Figure S2). Calnexin, an endoplasmic reticulum (ER) protein that acts as a negative EV marker was not detected during both purity and yield analyses. These results reflect the elimination of the majority of undesired plasma proteins by positive beads while retaining

EVs in solution preferably. Overall, we determined that the charge-based EV isolation method from blood plasma conducted at pH 7.4 can result in EV collection with high purity without compromising yield. Note that any fluctuations in EV stability were not also observed upon subjecting the EVs collected from the cell culture medium to the buffer-exchange steps involved in the charge-based EV isolation process (Figure S3).

To further verify the presence of EVs, the EV-containing supernatants isolated at pH 7.4 were subjected to nanoparticle tracking analysis (NTA) and examination by transmission electron microscopy (TEM). NTA results revealed that the supernatant sample being subjected to the charge-based isolation at pH 7.4 contained particles mainly in the size range from 50 to 200 nm (Figure 2e). In addition, nanoparticles with a cup-shaped morphology were observed by TEM, partially indicating the nature of particles as EVs (Figure 2f). The average zeta potential of the isolated EVs was found to be -10.2 mV (Figure S4).

To finally verify the efficacy of the developed charge-based EV collection method (Q), we compared its performance to those of popularly used conventional polymer precipitation (PP) and ultracentrifugation (UC) methods. A human plasma sample obtained from the same patient was equally divided for EV isolation by three different EV isolation methods. The CD63 purity analysis, which represents EV purity, by Western blotting revealed that the charge-based EV isolation method (Q) was superior to either PP or UC methods (Figure 3a). Indeed, a 2.5-fold and a 4-fold increase in CD63 purity were noted with the charge-based method compared to EV isolation by the PP and UC methods, respectively (Figure 3b). In addition, intensified bands for EV markers, including CD63, CD9, and TSG101 were noted for the plasma sample subjected to the charge-based EV isolation upon analyzing the yield of isolated EVs by Western blotting with equalized volume loading (Figure 3c). On the other hand, all three methods exhibited comparable amounts of albumin and demonstrated successful removal of HDLs. Although the charge-based and polymer precipitation EV isolation methods revealed LDL-associated ApoB-100 bands, unlike the UC method, no apparent CD63 and CD9 bands were observed in the UC method (Figure 3c). This means that the UC method is poor at yielding both EVs and contaminants, including lipoproteins (Figure 3c). The Western blot result is indeed in line with the EV yield measured by NTA which exhibited approximately 2 to 5 times higher yields of the charge-based EV isolation method (Q) in comparison to the PP and UC methods, respectively (Figure 3d). These results, therefore, further highlight the superior performance of the charge-based EV collection method in terms of EV purity and yield in comparison with conventional EV isolation methods.

4. CONCLUSION

The potential utilization of EVs in clinical applications for diagnostic and therapeutic purposes has highlighted the importance of the development of EV isolation methods that have been suboptimal. In line with this, we successfully developed a rapid, one-step charge-based EV collection method from blood plasma. By carefully controlling the buffer pH, we isolated EVs in superior purity and yield in comparison to conventional methods including UC and PP. Moreover, this method is rapid, taking only about 20 min including the buffer exchange step, and does not require a costly device as in the

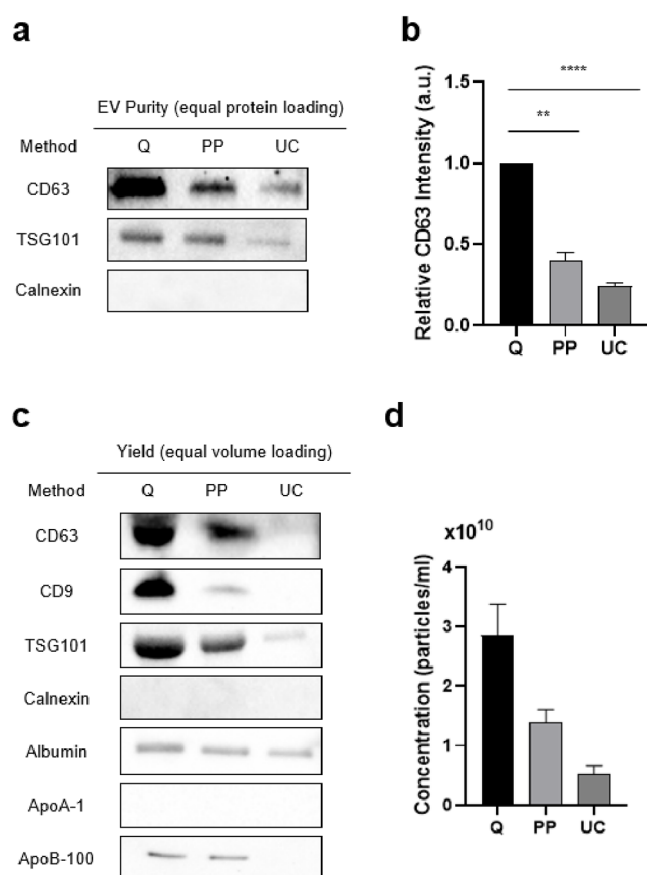


Figure 3. Comparing the performance of the charge-based EV isolation method to conventional methods. (a) Purity analysis of EVs collected using different isolation methods by Western blotting (CD63, CD9, and TSG101 (a negative EV marker)). (b) Relative CD63 band intensities obtained in (a) which indicate EV purity. (c) Yield analysis of EVs (CD63, CD9, TSG101, and calnexin (a negative EV marker)) and plasma impurities (albumin, HDLs (ApoA-1), and LDLs (ApoB-100)) by Western blotting which are found in the samples subjected to various EV isolation methods. (d) Yield analysis of EVs collected using various EV isolation methods by NTA. Data are means \pm s.e.m. [$n = 4$ for (a), (b), and (c), and $n = 3$ for (d)]; $**p < 0.001$, paired two-tailed Student's t test].

case of UC. We believe that the charge-based EV collection method would thus become a new EV isolation platform, thereby accelerating the clinical translation efforts in the field of EV research.

■ ASSOCIATED CONTENT

Supporting Information

The Supporting Information is available free of charge at <https://pubs.acs.org/doi/10.1021/acsomega.3c07427>

Surface charges of major plasma constituents and cell-line derived EVs, albumin and EV content (CD63) in unbound (UB, supernatant) and bead-bound (BD) fractions upon subjecting plasma to a charge-based EV isolation at pH 7.4, EV stability (measured in size) before and after buffer-exchange steps involved in the charge-based EV isolation method, and the average zeta potential of the EVs isolated with the developed charge-based method (Figures S1–S4) (PDF)

■ AUTHOR INFORMATION

Corresponding Author

Ji-Ho Park – Department of Bio and Brain Engineering and KAIST Institute for Health Science and Technology, Korea Advanced Institute of Science and Technology (KAIST), Daejeon 34141, Republic of Korea; orcid.org/0000-0002-0721-0428; Email: jihopark@kaist.ac.kr

Authors

Woojin Back – Department of Bio and Brain Engineering and KAIST Institute for Health Science and Technology, Korea Advanced Institute of Science and Technology (KAIST), Daejeon 34141, Republic of Korea

Minseo Bang – Department of Bio and Brain Engineering and KAIST Institute for Health Science and Technology, Korea Advanced Institute of Science and Technology (KAIST), Daejeon 34141, Republic of Korea

Jik-Han Jung – Department of Bio and Brain Engineering and KAIST Institute for Health Science and Technology, Korea Advanced Institute of Science and Technology (KAIST), Daejeon 34141, Republic of Korea

Ka-Won Kang – Division of Hematology-Oncology, Department of Internal Medicine, Korea University College of Medicine, Seoul 02841, Republic of Korea

Byeong Hyeon Choi – Department of Thoracic and Cardiovascular Surgery and Department of Biomedical Sciences, Korea University College of Medicine, Seoul 08308, Republic of Korea; Korea Artificial Organ Center, Korea University, Seoul 34141, Republic of Korea

Yeonho Choi – Department of Biomedical Engineering, Korea University, Seoul 02841, Republic of Korea; orcid.org/0000-0003-2018-3599

Sunghoi Hong – School of Biosystems and Biomedical Sciences, Korea University, Seoul 02841, Republic of Korea

Hyun Koo Kim – Department of Thoracic and Cardiovascular Surgery and Department of Biomedical Sciences, Korea University College of Medicine, Seoul 08308, Republic of Korea; orcid.org/0000-0001-7604-4729

Yong Park – Division of Hematology-Oncology, Department of Internal Medicine, Korea University College of Medicine, Seoul 02841, Republic of Korea

Complete contact information is available at:

<https://pubs.acs.org/10.1021/acsomega.3c07427>

Author Contributions

W.B. and J.-H.P. conceived and designed the research. W.B., M.B., J.-H.J., K.-W.K., and B.C. carried out the experiments. W.B., M.B., and J.-H.P. analyzed the data. Y.C., S.H., H.K.K., Y.P., and J.-H.P. provided project guidance. W.B. and J.-H.P. wrote and compiled the manuscript.

Notes

The authors declare no competing financial interest.

■ ACKNOWLEDGMENTS

This work was supported by the Basic Science Research Program through the National Research Foundation funded by the Ministry of Science and ICT, Republic of Korea (NRF-2021R1A2C2094074), and the Korea Health Technology R&D Project through the Korea Health Industry Development Institute funded by the Ministry of Health & Welfare, Republic of Korea (HR14C0007).

■ REFERENCES

- (1) D'Angelo, G.; Raposo, G. Shedding Light on the Cell Biology of Extracellular Vesicles. *Nat. Rev. Mol. Cell Biol.* **2018**, *19* (4), 213–228.
- (2) Raposo, G.; Stoorvogel, W. Extracellular Vesicles: Exosomes, Microvesicles, and Friends. *J. Cell Biol.* **2013**, *200* (4), 373–383.
- (3) Théry, C.; Zitvogel, L.; Amigorena, S.; Roussy, I. G. Exosomes: Composition, Biogenesis and Function. *Nat. Rev. Immunol.* **2002**, *2*, 569–579.
- (4) Caby, M.-P.; Lankar, D.; Vincendeau-Scherrer, C.; Raposo, G.; Bonnerot, C. Exosomal-like Vesicles Are Present in Human Blood Plasma. *Int. Immunol.* **2005**, *17* (7), 879–887.
- (5) Milasan, A.; Tessandier, N.; Tan, S.; Brisson, A.; Martel, C. Extracellular vesicles are present in mouse lymph and Their Level Differs in Atherosclerosis. *J. Extracell. Vesicles* **2016**, *5*, 31427.
- (6) Shenoy, G. N.; Loyall, J.; Berenson, C. S.; Kelleher, R. J.; Iyer, V.; Balu-Iyer, S. V.; Odunsi, K.; Bankert, R. B. Sialic Acid – Dependent Inhibition of T Cells by Exosomal Ganglioside GD3 in Ovarian Tumor Microenvironments. *J. Immunol.* **2018**, *201*, 3750–3758.
- (7) Manek, R.; Moghieb, A.; Yang, Z.; Kumar, D.; Kobessiy, F.; Sarkis, G. A.; Raghavan, V.; Wang, K. W. Protein Biomarkers and Neuroproteomics Characterization of Microvesicles/Exosomes from Human Cerebrospinal Fluid Following Traumatic Brain Injury. *Mol. Neurobiol.* **2018**, 6112–6128.
- (8) Aalberts, M.; Dissel-Emiliani, F. M. F.; Van Adrichem, N. P. H.; Van Wijnen, M.; Van Wauben, M. H. M.; Stout, T. A. E.; Stoorvogel, W. Identification Of Distinct Populations Of Prostatomes That Differentially Express Prostate Stem Cell Antigen, Annexin A1, And GLIPR2 In Humans. *Biol. Reprod.* **2012**, *86*, 82.
- (9) Herwijnen, M. J. C.; Van Zonneveld, M. I.; Goerdalay, S.; Nolte, E. N. M.; Garssen, J.; Stahl, B.; Altelaar, A. F. M.; Redegeld, F. A.; Wauben, M. H. M. Comprehensive Proteomic Analysis of Human Milk-Derived Extracellular Vesicles Unveils a Novel Functional Proteome Distinct from Other Milk Components * □. *Mol. Cell. Proteomics* **2016**, *15* (11), 3412–3423.
- (10) Kim, H. K.; Jo, W. M.; Jung, J. H.; Chung, W. J.; Shim, J. H.; Choi, Y. H.; Lee, I. S. Needleoscopic Lung Biopsy for Interstitial Lung Disease and Indeterminate Pulmonary Nodules: A Report on 65 Cases. *Ann. Thorac. Surg.* **2008**, *86* (4), 1098–1103.
- (11) Théry, C.; Witwer, K. W.; Aikawa, E.; Alcaraz, M. J.; Anderson, J. D.; Andriantsitohaina, R.; Antoniou, A.; Arab, T.; Archer, F.; Atkin-Smith, G. K.; et al. et al. Minimal Information for Studies of Extracellular Vesicles 2018 (MISEV2018): A Position Statement of the International Society for Extracellular Vesicles and Update of the MISEV2014 Guidelines. *J. Extracell. Vesicles* **2018**, *7*, 1535750.
- (12) Lötvall, J.; Hill, A. F.; Hochberg, F.; Buzás, E. I.; Vizio, D. D.; Gardiner, C.; Gho, Y. S.; Kurochkin, I. V.; Mathivanan, S.; Quesenberry, P.; et al. et al. Minimal Experimental Requirements for Definition of Extracellular Vesicles and Their Functions: A Position Statement from the International Society for Extracellular Vesicles. *J. Extracell. Vesicles* **2014**, *3*, 26913.
- (13) Witwer, K. W.; Buzás, E. I.; Bemis, L. T.; Bora, A.; Lässer, C.; Lötvall, J.; Nolte-t Hoen, E. N.; Piper, M. G.; Sivaraman, S.; Skog, J.; et al. et al. Standardization of Sample Collection, Isolation and Analysis Methods in Extracellular Vesicle Research. *J. Extracell. Vesicles* **2013**, *2*, 1.
- (14) Zhang, X.; Borg, E. G. F.; Liaci, A. M.; Vos, H. R. A Novel Three Step Protocol to Isolate Extracellular Vesicles from Plasma or Cell Culture Medium with Both High Yield and Purity. *J. Extracell. Vesicles* **2020**, *9*, 1791450.
- (15) Baranyai, T.; Herczeg, K.; Onódi, Z.; Voszka, I.; Módos, K.; Marton, N.; Nagy, G.; Mäger, I.; Wood, M. L.; Andaloussi, S.; et al. et al. Isolation of Exosomes from Blood Plasma: Qualitative and Quantitative Comparison of Ultracentrifugation and Size Exclusion Chromatography Methods. *PLoS One* **2015**, *10*, No. e0145686.
- (16) Welton, J. L.; Webber, J. P.; Botos, L. A.; Jones, M.; Clayton, A. Ready-Made Chromatography Columns for Extracellular Vesicle Isolation from Plasma. *J. Extracell. Vesicles* **2015**, *4*, 27269.
- (17) Yuana, Y.; Levels, J.; Grootemaat, A.; Sturk, A.; Nieuwland, R. Co-Isolation of Extracellular Vesicles and High-Density Lipoproteins

Using Density Gradient Ultracentrifugation. *J. Extracell. Vesicles* **2014**, *3*, 23262.

(18) Sódar, B. W.; Kittel, A. -; Pálóczi, K.; Vukman, K. V.; Osteikoeetxea, X.; Szabó-Taylor, K.; Németh, A.; Sperlágh, B.; Baranyai, T.; Giricz, Z.; et al. et al. Low-Density Lipoprotein Mimics Blood Plasma-Derived Exosomes and Microvesicles during Isolation and Detection. *Sci. Rep.* **2016**, *6*, 24316.

(19) Lobb, R. J.; Becker, M.; Wen, S. W.; Wong, C. S. F.; Wiegman, A. P.; Leimgruber, A.; Möller, A. Optimized Exosome Isolation Protocol for Cell Culture Supernatant and Human Plasma. *J. Extracell. Vesicles* **2015**, *4*, 27031.

(20) Onódi, Z.; Pelyhe, C.; Nagy, C. T.; Brenner, G. B.; Almási, L.; Kittel, A. -; Manček-Keber, M.; Ferdinandy, P.; Buzás, E. I.; Giricz, Z. Isolation of High-Purity Extracellular Vesicles by the Combination of Iodixanol Density Gradient Ultracentrifugation and Bind-Elute Chromatography from Blood Plasma. *Front. Physiol.* **2018**, *9*, 402695.

(21) Jung, J. H.; Back, W.; Yoon, J.; Han, H.; Kang, K. W.; Choi, B.; Jeong, H.; Park, J.; Shin, H.; Hur, W. Dual Size - Exclusion Chromatography for Efficient Isolation of Extracellular Vesicles from Bone Marrow Derived Human Plasma. *Sci. Rep.* **2021**, *11*, 217.

(22) Linares, R.; Tan, S.; Gounou, C.; Arraud, N.; Brisson, A. R. High-Speed Centrifugation Induces Aggregation of Extracellular Vesicles. *J. Extracell. Vesicles* **2015**, *4*, 29509.

(23) Garvey, W. T.; Kwon, S.; Zheng, D.; Shaughnessy, S.; Wallace, P.; Hutto, A.; Pugh, K.; Jenkins, A. J.; Klein, R. L.; Liao, Y. Effects of Insulin Resistance and Type 2 Diabetes on Lipoprotein Subclass Particle Size and Concentration Determined by Nuclear Magnetic Resonance. *Diabetes* **2003**, *52*, 453–462.

(24) Zhang, H.; Freitas, D.; Kim, H. S.; Fabijanic, K.; Li, Z.; Chen, H.; Mark, M. T.; Molina, H.; Martin, A. B.; Bojmar, L.; et al. et al. Identification of Distinct Nanoparticles and Subsets of Extracellular Vesicles by Asymmetric Flow Field-Flow Fractionation. *Nat. Cell Biol.* **2018**, *20*, 332–343.

(25) Sancho-Albero, M.; Navascués, N.; Mendoza, G.; Sebastián, V.; Arruebo, M. Exosome Origin Determines Cell Targeting and the Transfer of Therapeutic Nanoparticles towards Target Cells. *J. Nanobiotechnol.* **2019**, *17*, 1–13.

(26) Vlasova, I. M.; Sletsky, A. M. Study of the denaturation of human serum albumin by sodium dodecyl sulfate using the intrinsic fluorescence of albumin. *J. Appl. Spectrosc.* **2009**, *76* (4), 536–541.

(27) *Ion Exchange Chromatography*. <https://www.bio-rad.com/kokr/applications-technologies/ion-exchange-chromatography?ID=MWHAY9ESH>.

(28) Kowal, J.; Arras, G.; Colombo, M.; Jouve, M.; Paul, J.; Prindal-Bengtson, B. Proteomic Comparison Defines Novel Markers to Characterize Heterogeneous Populations of Extracellular Vesicle Subtypes. *Proc. Natl. Acad. Sci.* **2016**, *113*, No. E968–E977.

(29) Mathieu, M.; Névo, N.; Verweij, F. J.; Palmulli, R.; Rubinstein, E.; Boncompain, G.; Jouve, M.; Valenzuela, J. I.; Maurin, M.; Lankar, D.; et al. et al. Specificities of Exosome versus Small Ectosome Secretion Revealed by Live Intracellular Tracking of CD63 and CD9. *Nat. Commun.* **2021**, *12*, 4389.

(30) Li, M.; Huang, L.; Chen, J.; Ni, F.; Zhang, Y.; Liu, F. Isolation of Exosome Nanoparticles from Human Cerebrospinal Fluid for Proteomic Analysis. *ACS Appl. Nano Mater.* **2021**, *4*, 3351–3359.